

TC4 钛合金电子束焊接接头高温性能与组织

尹丽香¹, 许鸿吉¹, 魏志宇¹, 谢明¹, 王亚军²

(1. 大连交通大学 材料科学与工程学院, 辽宁 大连 116028; 2. 北京航空制造工程研究所, 北京 100024)

摘 要: 通过高温拉伸试验、高温持久拉伸试验以及金相分析对 TC4 钛合金电子束焊接接头的显微组织和高温性能进行了研究。结果表明, 用电子束焊接 TC4 钛合金可获得高温性能良好的焊接接头, 其焊接接头的高温抗拉强度为 630 MPa, 与母材相当。高温持久拉伸时焊接接头在 400 ℃ 下 100 h 的持久强度大于 600 MPa, 不低于 TC4 钛合金母材同等条件下的持久强度。TC4 钛合金母材室温下的组织为典型的轧制状态组织, 即拉长了的针状 $\alpha + \beta$ 组织, 焊缝组织是由原始 β 相转变而成的 α' 相, 即针状马氏体。经高温拉伸和高温持久拉伸后焊缝晶粒均明显长大, 但其晶粒的长大程度与高温持续时间无关。

关键词: TC4 钛合金; 电子束焊; 高温拉伸; 持久拉伸

中图分类号: TG457. 19 文献标识码: A 文章编号: 0253-360X(2007)10-049-04



尹丽香

0 序 言

TC4 钛合金(Ti-6Al-4V)是 20 世纪 50 年代发展起来的一种中等强度的 $\alpha - \beta$ 两相型钛合金, 它含有 6% α 稳定元素 Al 和 4% β 稳定元素 V。这种合金具有比重轻、比强度高、耐蚀性和高温抗蠕变性能等优异的综合性能, 因而在航空航天领域, 特别是航空发动机制造中得到了广泛的应用^[1-3]。此外, 该合金不仅室温抗拉强度极高, 而且具有足够的高温强度和高温抗氧化性能。因此, 自 20 世纪 80 年代以来, 在航海、海洋工程、化工、汽车制造和外科手术等领域的应用也越来越广泛^[4]。

随着航空发动机向大推力、高推重比、高可靠性等方向发展, 航空发动机结构越来越多地采用焊接结构。而 TC4 钛合金在保护良好的条件下可以采用钨极氩弧焊、熔化极惰性气体保护焊、等离子弧焊及电子束焊等多种方法进行焊接。由于 TC4 钛合金活性强, 熔化焊时需要用惰性气体或真空进行保护。真空电子束焊接具有能量密度高、穿透能力强、加热范围窄、焊接参数可调节范围宽、焊接速度快、焊接厚板时效率高、保护可靠等优点, 其应用范围和生产规模正日渐扩大, 在钛合金的焊接中也得到了广泛应用^[1, 5]。因此对 TC4 钛合金电子束焊接的研究工作也越来越受到国内外焊接工作者的重视。

1 试 验

试验材料为 TC4 钛合金板材, 板厚 14 mm, 固溶处理状态供货。采用真空电子束焊接, 焊接工艺参数如表 1 所示。焊后接头去应力退火。然后按航空标准进行高温拉伸和高温持久拉伸试验。高温拉伸试验按航空标准 HB5195-96 进行, 试样形式为螺纹圆形试样, 焊缝位于试样的中间。高温拉伸试验在 Instron 1196 电子万能试验机上进行, 试验温度为 400 ℃。高温持久拉伸试验按航空标准 HB5150-96 进行, 试样形状及尺寸见图 1, 焊缝位于试样的中间。持久拉伸试验在 BII-2 电子万能试验机上进行, 试验温度为 400 ℃。

表 1 TC4 钛合金真空电子束焊接工艺参数
Table 1 EB welding parameters of TC4 titanium alloy

	加速电压 U_a/kV	聚焦电流 I_f/mA	电子束电流 I_b/mA	焊接速度 $v/(m \cdot min^{-1})$
焊接过程	150	354	39	0.8
表面修饰	150	387	4	0.3

取高温拉伸及高温持久拉伸后试样中断裂位置距焊缝中心的距离较长的一段制成高温拉伸和持久拉伸焊接接头金相试样, 利用光学显微镜观察经高温拉伸和高温持久拉伸后焊接接头组织的变化, 并与室温焊缝组织进行对比分析温度对焊接接头组织的影响。

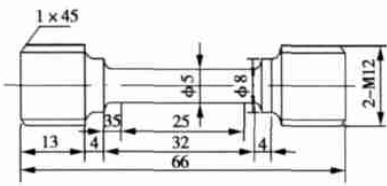


图 1 持久拉伸试样尺寸(mm)

Fig. 1 Dimension of endurant tensile test specimen

2 试验结果与分析

2.1 高温拉伸与持久拉伸试验结果

表 2 为 TC4 钛合金电子束焊接接头高温拉伸和

高温持久拉伸试验结果。从表 2 中可以看出, TC4 钛合金电子束焊接接头高温抗拉强度略低于母材, 断后伸长率和断面收缩率也很高。由于母材和焊接接头的断面收缩率均大于断后伸长率, 说明母材和焊接接头在高温拉伸时均有颈缩现象。TC4 钛合金电子束焊接接头的高温持久强度也略低于母材, 其 $\sigma_{100}^{400}>600\text{ MPa}$, 通过对高温拉伸和高温持久拉伸试样断裂部位的观察发现, TC4 钛合金电子束焊接接头高温拉伸和高温持久拉伸时断裂均发生在距焊缝中心较远的母材上, 这说明焊接接头与母材等强。因此采用电子束焊接 TC4 钛合金可获得高温性能良好的焊接接头。

TC4 钛合金母材及电子束焊接接头拉伸试样在高温拉伸及高温持久拉伸时均有颈缩现象, 焊接接

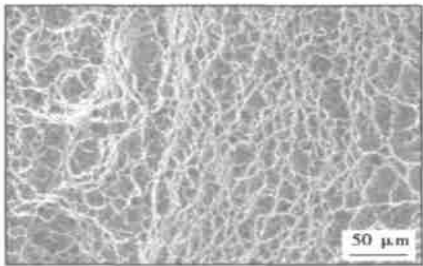
表 2 TC4 钛合金电子束焊接接头高温性能试验结果

Table 2 High-temperature mechanical properties of TC4 alloy EB welded joint

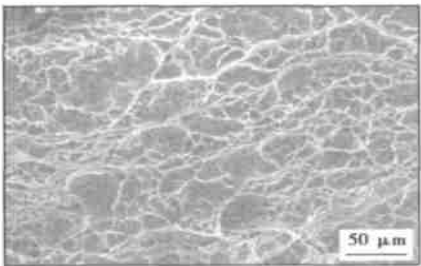
材料	试验温度 $T/^\circ\text{C}$	高温拉伸试验				高温持久拉伸		
		抗拉强度	规定非比例延伸强度	断后伸长率	断面收缩率	拉断部位	$\sigma_{100}^{400}/\text{MPa}$	拉断部位
		R_m/MPa	$R_{p0.2}/\text{MPa}$	$A(\%)$	$Z(\%)$			
母材	400	646.5	562.5	14.1	55.3	—	>620	—
接头	400	630	530.8	12.4	43.9	母材	>600	母材

头拉伸试样的颈缩区发生在母材上, 且母材的颈缩现象比焊接接头要明显。TC4 钛合金母材及电子束焊接接头高温拉伸和高温持久拉伸试样断口扫描图

像见图 2 和图 3。从图 2 和图 3 中看出, 高温拉伸及高温持久拉伸时 TC4 钛合金电子束焊接接头的断口形貌和母材的断口形貌大致相同, 均为浅韧窝。



(a) 母材



(b) 焊接接头

图 2 TC4 钛合金高温拉伸断口形貌

Fig. 2 Fracture appearances of TC4 alloy high-temperature tensile specimens

2.2 显微组织分析

室温下 TC4 钛合金母材组织为 α 相和 β 相的混合物, 针状 β 相均匀分布在 α 相基体上, 如图 4a 所示。通过扫描电镜观察 TC4 钛合金电子束焊接接头的显微组织发现, TC4 钛合金母材的轧制方向很明显, 组织为拉长的 $\alpha+\beta$ 相。焊缝组织是由较原始 β

相转变而成的 α' 相, 即针状马氏体(图 4b)。

TC4 钛合金电子束焊接接头经高温拉伸及持久拉伸后其焊缝晶粒明显长大, 如图 5 所示。从图 5 中可以看出, 焊接接头高温拉伸和持久拉伸后焊缝区的晶粒大小基本相同, 持续的高温并没有增大焊缝晶粒的长大趋势, 这说明焊缝晶粒在长大到一定程度时就

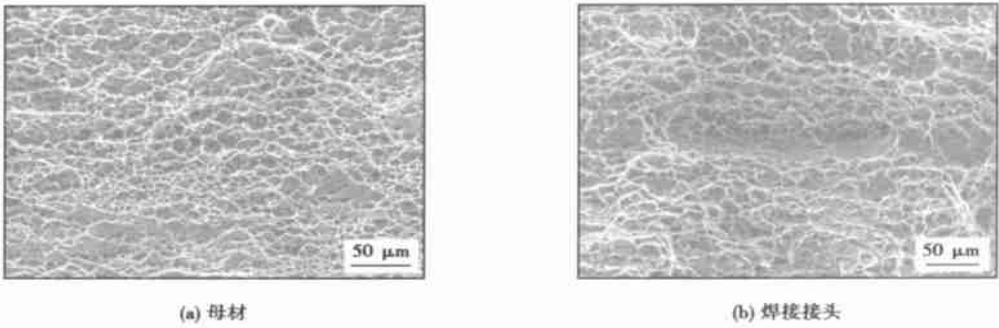


图 3 TC4 钛合金高温持久拉伸断口形貌
Fig. 3 Fracture appearances of TC4 alloy endurant tensile specimens

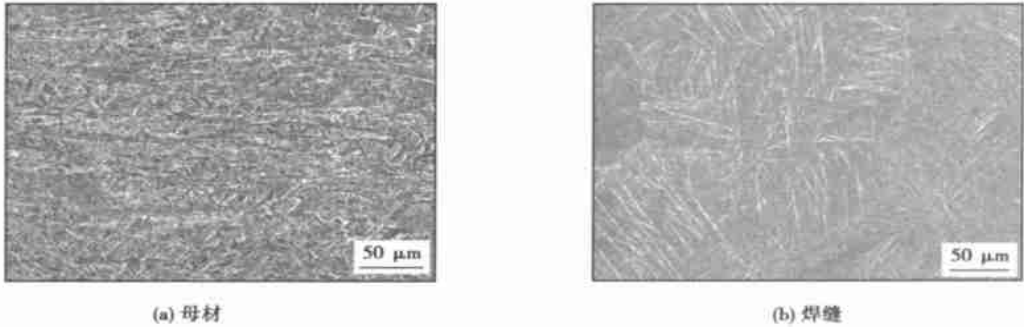


图 4 TC4 钛合金焊接接头显微组织
Fig. 4 Microstructure of TC4 alloy welded joint

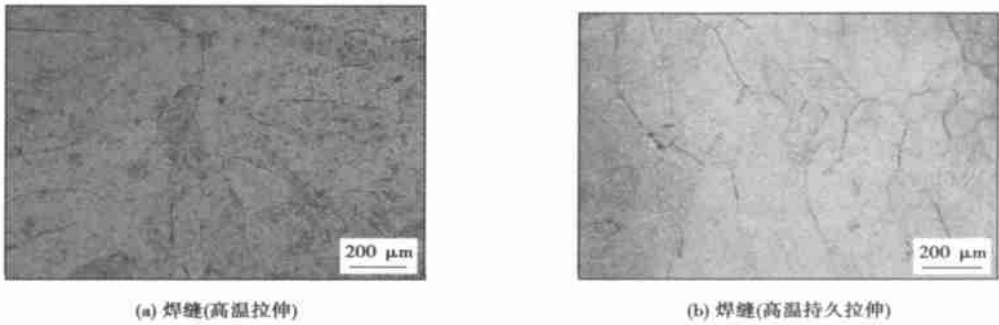


图 5 TC4 钛合金焊接接头高温拉伸及持久拉伸后焊缝组织
Fig. 5 Microstructure of TC4 alloy EB welded joint after high-temperature tensile test and endurant tensile test

不再长大,晶粒的长大程度与高温持续时间无关。

3 结 论

- (1) 400 ℃下 TC4 钛合金电子束焊接接头与母材等强,塑性相当。母材及电子束焊接接头高温拉伸试样的断口形貌均为浅韧窝。
- (2) TC4 钛合金电子束焊接接头具有较高的
高温持久强度,略低于母材。母材与电子束焊接接头
高温持久拉伸试样的断口形貌均为浅韧窝。

(3) TC4 钛合金在室温下的母材组织为典型的
轧制状态组织,即拉长了的针状 $\alpha + \beta$ 组织,焊缝组
织为针状马氏体 α' 相。高温拉伸及高温持久拉伸
后焊缝晶粒明显长大,但其长大程度与高温持续时
间无关。

参考文献:

[1] 胡礼木. 钛合金 Ti-6Al-4V 电子束焊接接头的性能研究[J] . 陕
西工学院学报, 1997, 13(4): 43- 47.

[2] 吴毅雄, 唐新华, 姚 舜. 精密连接技术及其在航空航天工业中的应用[C] // 中国机械工程学会焊接分会. 航空、航天焊接国际论坛论文集. 北京: 机械工业出版社, 2004: 152—158.

[3] 董宝明, 郭德伦, 张田仓. 钛合金焊接结构在先进飞机制造中的应用与发展[C] // 中国机械工程学会焊接分会. 航空、航天焊接国际论坛论文集. 北京: 机械工业出版社, 2004: 447—453.

[4] 李明怡. 航空用钛合金结构材料[J]. 世界有色金属, 2000(6): 17

—20.

[5] 张小明. 钛及钛合金的焊接[J]. 稀有金属快报, 2001(5): 17—20.

作者简介: 尹丽香 女, 1980 年出生, 硕士, 工程师。主要从事设备焊接工艺及无损检测要求的编制工作。发表论文 5 篇。

Email: lixiang.yin@hndeLED.com

[上接第 48 页]

[5] 阚前华, 谭长建, 张 娟, 等. ANSYS 高级工程应用实例分析与二次开发[M]. 北京: 电子工业出版社, 2006.

[6] 王 莉, 陈 旭, Nose H, 等. Anand 模型预测 63Sn37Pb 焊锡钎料的应力应变行为[J]. 机械强度, 2004, 26(4): 447—450.

[7] Basaran C, Desai C S, Kundu T. Thermal mechanical finite element analysis of problems in electronic packaging using the disturbed state concept[J]. ASEM Journal of Electronic Packaging, 1998, 120(2): 41—53.

[8] Lee S W, Zhang X. Sensitivity study on material properties for the fatigue life predication of solder joints under cyclic thermal loading[J].

Circuit World 1998 24(3): 26—31.

[9] 吴玉秀, 薛松柏, 张 玲, 等. QFP 组件的优化模拟及焊点热疲劳寿命的预测[J]. 焊接学报, 2006, 27(8): 99—102.

[10] 吴 敏. Ag 对 Sn-9Zn 合金钎料组织及性能的影响[J]. 电子元件与材料, 2006, 25(11): 34—35.

作者简介: 张 亮, 男, 1984 年出生, 硕士研究生。主要从事微电子焊接及无铅钎料研究。发表论文 1 篇。

Email: liang421064354@sina.com

on 45 steel substrate with the home-made special gas-filled-closed electric-spark deposition device and electric-spark deposition machine modeled DZ—1400, and the industry pure titanium (TA2) was used for electrode and the industry pure nitrogen for shielding and reactive gas. The phase of coatings was analyzed using X-ray diffractometer. The microstructure of coatings was investigated with scanning electron microscope. The microhardness of coatings was tested by hardness-testing device. The wear-resisting property of coatings was compared with that of W18Cr4V rapid steel treated by quenching using the home-made abrasion machine. The results indicated that excellent bonding between the coating and the carbon steel substrate is ensured by the strong metallurgical interface. The coatings was mainly made up of Ti coming from electrode, TiN ceramic particle synthesized in-situ and Fe coming from substrate. The average microhardness of coating is 1 323 HV0.1 and its wear-resisting property is better than that of W18Cr4V rapid steel treated by quenching.

Key words: electric-spark deposition; reactive synthesis; TiN; composite coating

Analysis for local incomplete brazing in fusion-brazed joints between aluminium and zinc coated steel by hybrid welding

LEI Zhen, QIN Guoliang, WANG Xuyou, LIN Shangyang (Harbin Welding Institute, China Academy of Machinery Science and Technology, Harbin 150080, China), p37—40, 44

Abstract: The cause of the local incomplete brazing at the root of the bond line of the fusion-brazed joint between aluminium and steel was studied, and the relevant measures were developed to restrain or avoid the defect. Analysis results showed that insufficient heat input is the essential cause to form the local incomplete brazing defect, and the temperature of the molten pool and the steel sheet at the root of the bond line can not reach the critical brazing temperature to achieve a brazing joint using Al-Si brazing filler metal which is the direct reason of local incomplete brazing. Moreover the local incomplete brazing is indirectly influenced by the fluid flow of the molten pool and the heat dissipation of base metals. The local incomplete brazing defect can be restrained or avoided by increasing the heat input or adjusting the location of the laser spot and arc.

Key words: laser; plus metal inert-gas arc; hybrid welding; fusion-brazing joining; local incomplete brazing

Welding identifying strategy based on sharing control in force tele-teaching

LIU Lijun^{1,2}, DAI Hongbin², GAO Hongming³, WU Lin³ (1. Ningbo Institute of Technology, Zhejiang University, Ningbo 315100, Zhejiang, China; 2. School of Material Science & Engineering, Harbin University of Science and Technology, Harbin 150080, China; 3. State Key Laboratory of Advanced Welding Production Technology, Harbin Institute of Technology, Harbin 150001, China), p41—44

Abstract: The tele-teaching was achieved by the shared technology in some cases, such as the probe locked by complex curve welding seam, and turning point. A welding seam identifying plat was founded based on the shared control in tele-teaching. The shared control mainly makes the operator in cooperate with robot to ensure the operating mode to transform smoothly, and the control in-

struction to superimpose in real-time. Sharing control mode was defined in tele-teaching. The control right between operator and remote robot is effectively shared by self-adjusting teaching and manual adjusting control. Tele-teaching experiment of half-box workpiece on shared control was completed. The experimental results show that the position precision of tele-teaching-playback is less than ± 0.5 mm, which can meet remote welding process.

Key words: remote welding; tele-teaching; force; shared technology; welding identifying

Finite element analysis on soldered joint reliability of QFP device with different solders

ZHANG Liang, XUE Songbai, LU Fangyan, HAN Zongjie (College of Materials Science and Technology, Nanjing University of Aeronautics and Astronautics, Nanjing 210016, China), p45—48, 52

Abstract: Finite element method was used to study the reliability of soldered joints of QFP device with three kinds of solders. The results indicate that the strain concentration areas in soldered joint locates at the heel and toe of the soldered joint and the area between the lead and soldered joint. Comparing with the simulating results about Sn3.8Ag0.7Cu, Sn9Zn and Sn63Pb37, from the diagrams of equivalent stress curves, it is found that the stress value in the soldered joint with Sn63Pb37 solder is the largest, and the value in the joint with Sn3.8Ag0.7Cu solder is the least. Sn3.8Ag0.7Cu is considered one of the most favorable solder as a lead-free standard alloy for packaging of micro-devices. By analyzing stress diagrams of curves of solder of the two kinds of QFP64 and QFP208 devices, the stress of solder of QFP208 is lower than that of QFP64, so its reliability is better.

Key words: finite element method; reliability; micro-devices; stress diagrams

Microstructures and high-temperature properties of TC4 titanium alloy joints welded by electron beam

YIN Lixiang¹, XU Hongji¹, WEI Zhiyu¹, XIE Ming¹, WANG Yajun² (1. School of Materials Science and Engineering, Dalian Jiaotong University, Dalian 116028, China; 2. Beijing Aeronautical Manufacturing Technology Research Institute, Beijing 100024, China), p49—52

Abstract: The microstructures and high-temperature properties of TC4 titanium alloy joints welded by the electron beam were investigated by high-temperature tensile test, high-temperature endurant tensile test and metallographic examination. The results showed that the joint of TC4 alloy with good performance at high-temperature can be obtained by means of electron beam welding. The high-temperature tensile strength of welded joint was 630 MPa, almost the same with that of the base metal. The endurant tensile strength of welded joint under 400 °C for 100 h was greater than 600 MPa, not less than that of the base metal. The microstructure of the weld is α' phase (needle martensite) which is transformed from the primary β matrix. The grain size of the weld which were obtained after high-temperature tensile test and high-temperature endurant tensile test becomes larger than that of weld at room-temperature, but the growth degree of the grain was not dependent on the high-temperature duration.

Key words: TC4 titanium alloy; electron beam welding;

high-temperature tensile test; endurant tensile test

Welding process of micro-alloying cast iron electrode ZHAI Qiuya, ZHAI Bo, TANG Zhen, XU Jinfeng (School of Materials Science and Engineering, Xi'an University of Technology, Xi'an 710048, China). p53—56

Abstract: Using a micro-alloying cast iron electrode the relationship between preheat temperature and microstructure and properties of joint were investigated by backing welding with low-current and then continuous welding with high-current. The results showed that the micro-alloying cast iron electrode has strong graphitizing ability and the weld metal had a little chilling tendency. The applied welding process can effectively decrease the depth of fusion zone and suppress the precipitation of cementite in fusion zone at a great extent. Thus the welding with the micro-alloying cast iron electrode can be realized at ambient temperature. When the preheated temperature is less than 200 °C, the homogeneous weld can be obtained which has the same microstructure and properties as base metal. With the increase of the preheat temperature, the graphite morphology in weld changes from spotted graphite to rosette graphite to flake graphite. The contents of graphite and ferrite increase while the hardness of the weld decreases. If the preheated temperature reaches to 200 °C, the microstructure of the weld consists of pearlite, ferrite, flake graphite and rosette graphite, and the microstructure of fusion zone consists of pearlite, small shiver ferrite and undercooled graphite. The welded joint has excellent mechanical properties.

Key words: micro-alloying cast iron electrode; iron casting; ambient temperature welding; microstructure and properties of joint

Analysis of characteristic of vertical position laser welding for aluminum alloys MIAO Yugang, CHEN Yanbin, LI Liqun, WU Lin (State Key Laboratory of Advanced Welding Production Technology, Harbin Institute of Technology, Harbin 150001, China). p57—60

Abstract: The experiments of vertical and flat position laser welding for 4 mm-thick 5A06 aluminum alloys were implemented, and the characteristics of weld dimension and porosity in the vertical position laser welding for aluminum alloys were investigated. The results show that the concave value and excessive penetration value of vertical welding is less than those of flat welding. Further, with the increase of heat input, the difference of vertical and flat welding becomes obvious. The weld appearance and dimension of the vertical welding and flat welding were slightly different. When the heat input is increased to a great extent, the weld depth of vertical welding is more than that of flat welding. However, the weld width of vertical welding is less than that of flat welding. The porosity of vertical position laser welding for aluminum alloys is composed of the large and irregular porosity or hole. It is not obviously different during vertical welding and flat welding, and a great deal of porosity concentrates in the upper and middle part of weld section, which can be indicated from the distributing position and shape of porosity. The number of porosity in vertical welding was slightly less than that of flat welding for the same welding parameters.

Key words: aluminum alloys; vertical position laser welding; flat welding; characteristic

Effect of aluminizing and diffusion treatment on adhesive strength of arc sprayed coatings WANG Qiang, LAN Dongyun, XUAN Zhaozhi, LIU Chenghui (College of Materials Science and Engineering, Jilin University, Changchun 130025, China). p61—64

Abstract: Corrosion-resisting and heat-resisting coatings of 18-8 stainless steel were made by arc spraying, aluminizing and diffusion treatment on cast iron. The microstructures and chemical compositions of coatings with aluminizing and diffusion treatment were studied by optical microscope, scanning electron microscope and X-ray diffraction. And the adhesive strength of coatings was evaluated by thermal fatigue tests. The results show that there are some regions with metallurgy bonding on the interface between coatings and substrates through aluminizing and diffusion treatment, therefore, the adhesive strength of coatings were improved greatly. And a long period of aluminizing time is adverse to the adhesive strength of coatings, so aluminizing time should be controlled well.

Key words: arc spraying; aluminizing; diffusion; adhesive strength

Microstructure and melting property of Sn-2.5Ag-0.7Cu-XGe solder MENG Gongge¹, YANG Tuoyu², CHEN Leida¹ (1. School of Material Science & Engineering, Harbin University of Science and Technology, Harbin 150040, China; 2. Anhui Science and Technology University, Bengbu 233100, Anhui, China). p65—68

Abstract: The 3 composition Sn-2.5Ag-0.7Cu-XGe lead-free solders were studied by scanning electron microscope and differential scanning calorimetry equipments. The result indicates that the microstructure is cobblestone-like pro-eutectic grain and scattered long narrow piece and small pellet eutectic mixture. With 0.5% or 1.0% element Ge, the microstructure morphology does not change. But the intermetallic compounds of Ag₃Sn and Cu₆Sn₅ tend to be fine, and their dispersion tends to be well-distributed, and Ag₃Sn phase tends to be fine needle from long narrow piece. By adding element Ge, the temperatures of the melting beginning, the melting peak and the melting finish all reduce correspondingly. And in the melting curve, the endothermic peak changes is narrow, and the melting finish part is long, but the melting temperature zone varies a little.

Key words: lead-free solder; microstructure; melting property

Solidification cracking mechanism of 690 nickel-based alloy surfacing metal BO Chunyu, YANG Yuting, CHOU Shuguo, ZHOU Shifeng (Harbin Welding Institute, China Academy of Machinery Science and Technology, Harbin 150080, China). p69—72

Abstract: Transverse restraint test was used to investigate the solidification cracking mechanism of 690 nickel-based alloy surfacing metal. Results show that the solidification cracking susceptibility of 690 nickel-based alloy surfacing metal is closely correlated with the segregation process during welding, which is greatly influenced by Nb. The solidification temperature of 690 nickel-based alloy surfacing metal falls when the Ni, Nb-rich phases segregate on the grain boundary or subgrain boundary, which induces that the ductility decreases and the appearance is fined. Then, cracking initiates and